

Mathematical Modelling of Chemical Clock Reactions. I. Induction, Inhibition and the Iodate--Arsenous-Acid Reaction

J. Billingham and D. J. Needham

Phil. Trans. R. Soc. Lond. A 1992 **340**, 569-591

doi: 10.1098/rsta.1992.0080

Email alerting service

Receive free email alerts when new articles cite this article - sign up in the box at the top right-hand corner of the article or click [here](#)

To subscribe to *Phil. Trans. R. Soc. Lond. A* go to:
<http://rsta.royalsocietypublishing.org/subscriptions>

Mathematical modelling of chemical clock reactions. I. Induction, inhibition and the iodate–arsenous-acid reaction

BY J. BILLINGHAM¹ AND D. J. NEEDHAM²

¹*Schlumberger Cambridge Research, High Cross, Madingley Road, Cambridge CB3 0EL, U.K.*

²*School of Mathematics, University of East Anglia, Norwich NR4 7TJ, U.K.*

Contents

1. Introduction	569
2. Two simple model clock reactions	570
(a) Cubic autocatalysis	570
(b) A simple model with an inhibitor	571
3. Indirect autocatalysis with an inhibitor: the iodate–arsenous-acid reaction	577
(a) Asymptotic solution of the initial-value problem for $0 < \epsilon \ll 1$ with $\delta = O(\epsilon)$ and $K = O(1)$	583
(b) Asymptotic solution of the initial-value problem for $K \gg 1$ with $\epsilon, \delta = O(1)$	586
(c) Asymptotic solution of the initial-value problem for $0 < \epsilon \ll 1, K \gg 1$	589
4. Conclusion	590
References	591

A clock reaction is a chemical reaction that gives rise to an initial induction period before a significant concentration of one of the chemical species involved is produced. We study three isothermal model reaction schemes that can exhibit clock reaction behaviour in a well-stirred situation. We also identify two types of reaction mechanism that can lead to clock reaction behaviour and indicate which is dominant in each of the model systems that we study. These include a well-known model of the iodate–arsenous-acid reaction.

1. Introduction

During a chemical clock reaction the concentration of one of the chemical species involved (the clock chemical) has the following distinguishing features.

(a) After the initial mixing of the reactants there is an induction period during which the concentration of the clock chemical is low.

(b) At the end of this induction period the concentration of the clock chemical increases, often very rapidly.

Typical examples of such reactions are the iodate–arsenous-acid reaction (Hanna *et al.* 1982), the iodine–bisulphate clock (Lambert & Fina 1984), the formaldehyde clock (Jones & Oldham 1963), the hydration of carbon dioxide (Jones *et al.* 1964), and

Phil. Trans. R. Soc. Lond. A (1992) **340**, 569–591

© 1992 The Royal Society and the authors

Printed in Great Britain

569

the oxidation of luminol by hydrogen peroxide (Candy *et al.* 1992), all of which are solution phase reactions. If a suitable indicator is added to the reaction mixture, the end of the induction period is marked by a sudden colour change or, in chemiluminescent reactions such as the oxidation of luminol, a flash of light. As a consequence, clock reactions are often used as demonstrations of chemical kinetics for undergraduates (Haggett *et al.* 1963) and as tricks in ‘chemical magic shows’ (Barrett 1955). A more important class of reactions that can exhibit an induction period is that of chain reactions (Dainton 1966). These include the photosynthesis of hydrogen chloride in the presence of ammonia, the photopolymerization of vinyl acetate in the presence of benzoquinone (Burnett & Melville 1947) and the atmospheric oxidation of a variety of organic substances (Scott 1965). This type of reaction often forms the basis of an industrial process, when it is vital to be able to control, or at least predict, the length of the induction period.

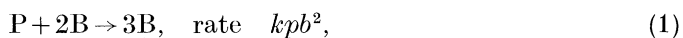
In this paper we study three model, isothermal reaction schemes in a closed, well-stirred reaction vessel, all of which can exhibit clock behaviour for certain ranges of parameter values. In §2 we identify two distinct mechanisms that can lead to clock behaviour and analyse two simple model systems based on these mechanisms. In §3 we study a more complex system that is a combination of those analysed in §2. This model is well known, and is in good qualitative and quantitative agreement with the kinetics of both the iodate–arsenous-acid reaction and the iodine–bisulphate clock reaction. We provide a thorough analysis of the second-order autonomous system of differential equations which describe the time evolution of the chemical concentrations. In particular, we show that clock behaviour can arise from either of the two mechanisms described in §2, depending upon the initial concentrations of the reactants.

The analytical methods adopted in the paper provide a general approach for examining model kinetic schemes for the possibility of clock reaction behaviour. When clock reaction behaviour is present, simple analytical expressions are obtained for the induction and inhibition periods, and the evolutionary structure of the reaction is uncovered.

2. Two simple model clock reactions

(a) *Cubic autocatalysis*

Autocatalytic reaction steps form the basis of many successful models of chemical reactions, for example the Belousov–Zhabotinskii reaction (Field & Noyes 1974), the hydroxylamine–nitric-acid reaction (Gowland & Stedman 1983), the hydrogen–oxygen and carbon-monoxide–oxygen reactions (Gray *et al.* 1984) and, as we shall discuss in detail in §3, the iodate–arsenous acid reaction and the iodine–bisulphate clock reaction. Here, we consider cubic autocatalysis,



where P is a reactant and B is the autocatalyst with concentrations p and b respectively, and k is a reaction rate constant. This simple reaction scheme has been investigated extensively both in a continuous flow, stirred tank reactor (see, for example, Gray & Scott 1983) and an unstirred reaction vessel where diffusion acts on the chemical species P and B (see, for example, Billingham & Needham 1991). For the purposes of this paper we simply consider cubic autocatalysis in a closed, well-stirred reaction vessel with initial concentrations $p = p_0$ and $b = b_0$. The reaction rate

equations are $dp/dt = -kpb^2$ and $db/dt = kpb^2$, where t is time. We define dimensionless variables by

$$\beta = b/p_0, \quad \gamma = p/p_0, \quad \tau = kp_0^2 t. \quad (2a)$$

in terms of which the reaction rate equations become

$$d\gamma/d\tau = -\gamma\beta^2, \quad d\beta/d\tau = \gamma\beta^2, \quad (2b)$$

subject to the initial conditions

$$\gamma(0) = 1, \quad \beta(0) = \epsilon, \quad (2c)$$

where $\epsilon = b_0/p_0$ is the dimensionless initial concentration of the autocatalyst, B. The solution of the initial-value problem (2) is readily obtained as

$$\gamma = 1 + \epsilon - \beta, \quad \tau = \frac{1}{(1 + \epsilon)^2} \left[\ln \left\{ \frac{\beta}{\epsilon(1 + \epsilon - \beta)} \right\} + \frac{(1 + \epsilon)(\beta - \epsilon)}{\epsilon\beta} \right]. \quad (2d)$$

This shows that $\beta \rightarrow (1 + \epsilon)$, $\gamma \rightarrow 0$ as $\tau \rightarrow \infty$, so that the autocatalyst, B, consumes all of the reactant, P, as we would expect. However, if the initial concentration of the autocatalyst, B, is small compared with the initial concentration of the reactant, P, so that $0 < \epsilon \ll 1$, there is an induction period before the concentration, β , increases significantly. By analysing the exact solution (2d) we find that for $0 < \epsilon \ll 1$ the solution develops in two asymptotic regions, with

$$\beta = \frac{\epsilon}{1 - \hat{\tau}} + O(\epsilon^2), \quad \gamma = 1 - \frac{\epsilon\hat{\tau}}{1 - \hat{\tau}} + O(\epsilon^2), \quad \text{as } \epsilon \rightarrow 0, \quad \text{with } \hat{\tau} = O(1), \quad (3a)$$

where $\hat{\tau} = \epsilon\tau$. The expansions (3a) become non-uniform when $\hat{\tau} = 1 - \epsilon \ln \epsilon + O(\epsilon)$, and we have

$$\beta = \beta_0(T) + O(\epsilon), \quad \gamma = 1 - \beta_0(T) + O(\epsilon), \quad (3b)$$

as $\epsilon \rightarrow 0$, with

$$T = O(1), \quad T < 0, \\ T \geq O(1), \quad T > 0,$$

where $T = (\hat{\tau} - 1 + \epsilon \ln \epsilon) \epsilon^{-1}$. The function $\beta_0(T)$ is defined implicitly by

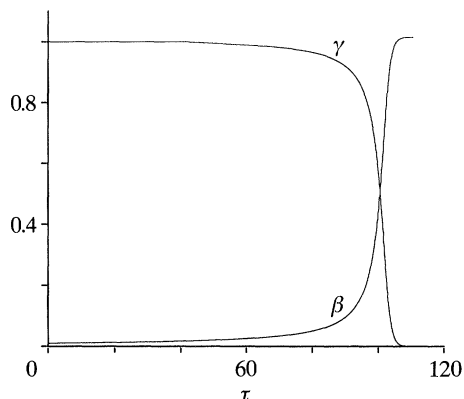
$$\ln \left[\frac{\beta_0}{1 - \beta_0} \right] - \frac{1}{\beta_0} - 1 - T = 0. \quad (3c)$$

Expansions (3b) remain uniform as $T \rightarrow +\infty$. Thus, for $\epsilon \ll 1$, cubic autocatalysis in a well-stirred system is a clock reaction with a well defined induction period of duration $\tau = \tau_0$, where $\tau_0 = \epsilon^{-1} - \ln \epsilon + O(1)$, as $\epsilon \rightarrow 0$. A graph of the solution (2d) is illustrated in figure 1 for $\epsilon = 0.01$, which clearly shows the changes in β and γ that occur when $\tau = \tau_0 \approx 100$ in this case. In terms of the physical variables we have shown that for $0 < b_0 \ll p_0$, cubic autocatalysis in a well-stirred system is a clock reaction with an induction period of duration $t_0 \approx 1/k_0 p_0 b_0$.

(b) *A simple model with an inhibitor*

In this section we study the system



Figure 1. The solution (2d) for $\epsilon = 0.01$.

where C is an inhibitor and D is an inert product with concentrations c and d respectively, and k_0 and k_1 are reaction rate constants. If the reaction step (4b) typically proceeds much more rapidly than step (4a), the system models a clock reaction. The induction period is caused by the rapid consumption of the clock chemical, B, by the inhibitor, C, which keeps the concentration of B low until C is completely consumed. The reaction step (4a) then causes the concentration of B to increase. The presence of an inhibitor can be used to explain the behaviour of many of the reactions listed in the introduction.

The reaction rate equations for the concentrations p , b and c are

$$dp/dt = -k_0 p, \quad db/dt = k_0 p - k_1 bc, \quad dc/dt = -k_1 bc. \quad (5a-c)$$

The concentration, d , of the inert product, D, is then determined by conservation of matter as, $d = c_0 - c$, where we have assumed that the species B and D are not present initially so that, $p = p_0$, $b = 0$, $c = c_0$, $d = 0$, at $t = 0$. Equation (5a) can be integrated immediately to give

$$p = p_0 e^{-k_0 t}. \quad (6a)$$

By subtracting equation (5c) from equation (5b) and integrating once we obtain $c = b - p_0(1 - e^{-k_0 t}) + c_0$, and hence arrive at a single first order ordinary differential equation for b , namely,

$$db/dt = k_0 p_0 e^{-k_0 t} - k_1 b \{b - p_0(1 - e^{-k_0 t}) + c_0\}. \quad (6b)$$

It is now convenient to define dimensionless variables by, $\beta = b/c_0$, $\gamma = c/c_0$, $\tau = k_0 p_0 t/c_0$, in terms of which equation (6b) becomes

$$\gamma = \beta - \epsilon^{-1}(1 - e^{-\epsilon\tau}) + 1, \quad (7a)$$

$$d\beta/d\tau = e^{-\epsilon\tau} - K\beta\{\beta - \epsilon^{-1}(1 - e^{-\epsilon\tau}) + 1\}. \quad (7b)$$

The dimensionless parameters ϵ and K are defined by,

$$\epsilon = c_0/p_0, \quad K = k_1 c_0^2/k_0 p_0, \quad (8)$$

where ϵ is the dimensionless initial concentration of the inhibitor, C, and K is a measure of the typical reaction rate of the step (4b) relative to that of (4a). We require a solution of the Riccati equation (7b) subject to the initial condition

$$\beta(0) = 0, \quad (9a)$$

which is readily obtained as

$$\beta = \epsilon^{-1}(1 - e^{-\epsilon\tau}) - 1 + \frac{\exp[K\{(1 - \epsilon^{-1})\tau + \epsilon^{-2}(1 - e^{-\epsilon\tau})\}]}{K \int_0^\tau \exp[K\{(1 - \epsilon^{-1})s + \epsilon^{-2}(1 - e^{-\epsilon s})\}] ds + 1}, \quad (9b)$$

after which (7a) becomes

$$\gamma = \frac{\exp[K\{(1 - \epsilon^{-1})\tau + \epsilon^{-2}(1 - e^{-\epsilon\tau})\}]}{K \int_0^\tau \exp[K\{(1 - \epsilon^{-1})s + \epsilon^{-2}(1 - e^{-\epsilon s})\}] ds + 1}. \quad (9c)$$

This solution was first obtained by Chien (1948) who studied the reaction scheme (4a, b) but made no attempt to analyse the qualitative form of the solution (9b, c), which is not immediately obvious. It is, however, clear from (9b, c) that

$$\beta \rightarrow \epsilon^{-1} - 1, \quad \gamma \rightarrow 0 \quad \text{as } \tau \rightarrow \infty \quad (0 \leq \epsilon \leq 1), \quad (10a)$$

$$\beta \rightarrow 0, \quad \gamma \rightarrow 1 - \epsilon^{-1} \quad \text{as } \tau \rightarrow \infty \quad (\epsilon > 1). \quad (10b)$$

In terms of the physical variables, if $\epsilon \leq 1$ ($p_0 \geq c_0$) the precursor, P, is in excess over the inhibitor chemical, C, so that C is completely consumed, whilst if $\epsilon > 1$, ($c_0 > p_0$) the initial concentration of P is not large enough to consume all of the inhibitor chemical, C.

We now examine the solution (9b, c) under the additional assumption that the precursor chemical, P, is initially in large excess over the inhibitor chemical, C, so that $0 < \epsilon \leq 1$. We expand β and γ as

$$\left. \begin{aligned} \beta(\tau; \epsilon, K) &= \beta_I(\tau; K) + o(1), \\ \gamma(\tau; \epsilon, K) &= \gamma_I(\tau; K) + o(1) \quad \text{as } \epsilon \rightarrow 0 \quad \text{with } \tau = O(1). \end{aligned} \right\} \quad (11a)$$

After substituting these expansions into equations (7a, b) we obtain the leading order problem

$$\gamma_I = \beta_I - \tau + 1, \quad d\beta_I/d\tau = 1 - K\beta_I(\beta_I - \tau + 1), \quad \beta_I(0) = 0. \quad (11b-d)$$

The solution of the initial-value problem (11c, d) is readily obtained as

$$\beta_I = \tau - 1 + \frac{e^{-\frac{1}{2}K(\tau-1)^2}}{K \int_0^\tau e^{-\frac{1}{2}K(s-1)^2} ds + e^{-\frac{1}{2}K}}, \quad \gamma_I = \frac{e^{-\frac{1}{2}K(\tau-1)^2}}{K \int_0^\tau e^{-\frac{1}{2}K(s-1)^2} ds + e^{-\frac{1}{2}K}}, \quad (12a, b)$$

which is clearly the limiting form of the solution (9b, c) as $\epsilon \rightarrow 0$ with $\tau = O(1)$. From (12a, b),

$$\beta_I(\tau; K) \sim \tau - 1 + c_\infty(K) e^{-\frac{1}{2}K(\tau-1)^2}, \quad \gamma_I(\tau; K) \sim c_\infty(K) e^{-\frac{1}{2}K(\tau-1)^2}, \quad (13a, b)$$

as $\tau \rightarrow \infty$, with

$$c_\infty(K) = \left[K \int_0^\infty e^{-\frac{1}{2}K(s-1)^2} ds + e^{-\frac{1}{2}K} \right]^{-1}, \quad (13c)$$

and we note that $c_\infty(K) \sim K^{-\frac{1}{2}}/\sqrt{2\pi}$, as $K \rightarrow \infty$.

The solution (12a, b) is not in agreement with (10a) as $\tau \rightarrow \infty$, which indicates that expansions (11a) must become non-uniform as $\tau \rightarrow \infty$. An examination of the full solution (9b, c) then shows that this non-uniformity arises when $\tau = O(\epsilon^{-1})$. We can

regard the expansions (11a) as the inner solution and now construct an outer solution, valid when $\tau = O(\epsilon^{-1})$, as $\epsilon \rightarrow 0$. The leading order inner solution (12a, b) shows that $\beta_I = O(\epsilon^{-1})$ and γ_I is exponentially small when $\tau = O(\epsilon^{-1})$. Appropriate scaled variables are therefore, $T = \epsilon\tau$, $B = \epsilon\beta$, $\gamma = o(\epsilon^n) \forall n > 0$, as $\epsilon \rightarrow 0$. After writing equation (7b), in terms of these variables, we expand B as,

$$B(T; \epsilon, K) = \sum_{n=0}^{\infty} \epsilon^n B_{\text{out}}^{(n)}(T; K) + E(T; K) \quad \text{as } \epsilon \rightarrow 0 \quad \text{with } T = O(1), \quad (14a)$$

and $E(T; K) = o(\epsilon^n)$ for all $n > 0$. On substituting into the scaled equation and solving at each order (subject to matching with the inner expansion (11a) as $T \rightarrow 0$) we readily find that

$$B_{\text{out}}^{(0)} = 1 - e^{-T}, \quad B_{\text{out}}^{(1)} = -1, \quad B_{\text{out}}^{(n)} \equiv 0 \quad \text{for } n = 2, 3, \dots \quad (14b)$$

Finally, we obtain the equation

$$dE/dT = -(K/\epsilon^2)(1 - e^{-T} - \epsilon)E \quad (14c)$$

for the exponentially small term in (14a). An integration of (14c) readily gives

$$E(T; K) = \epsilon c_{\infty}(K) \exp[-(K/\epsilon^2)(T - 1 + e^{-T} - \epsilon T + \frac{1}{2}\epsilon^2 + O(\epsilon^3))] \quad (14d)$$

after matching to (13a). Thus we have in the outer region, via (14a-d),

$$\left. \begin{aligned} \beta(\tau; \epsilon, K) &= \epsilon^{-1}(1 - e^{-T}) - 1 + c_{\infty}(K) \exp[-(K/\epsilon^2)(T - 1 + e^{-T} - \epsilon T + \frac{1}{2}\epsilon^2 \\ &\quad + O(\epsilon^3))] + \dots, \\ \gamma(\tau; \epsilon, K) &= c_{\infty}(K) \exp[-(K/\epsilon^2)(T - 1 + e^{-T} - \epsilon T + \frac{1}{2}\epsilon^2 + O(\epsilon^3))] + \dots, \end{aligned} \right\} \quad (14e)$$

as $\epsilon \rightarrow 0$ with $T = O(1)$. These expansions are in agreement with (10a) as $T \rightarrow \infty$, and complete the asymptotic solution of the initial-value problem (7b), (9a) for $0 < \epsilon \ll 1$.

We now investigate the possibility of clock reaction behaviour in the solution of the inner problem (12a, b). We expect that this type of behaviour arises when the reaction step (4b) typically proceeds much faster than the reaction step (4a), so that $K \gg 1$. We can determine the asymptotic structure of the solution (12a, b) via Laplace's method. However, this structure can be analysed more effectively by using the method of matched asymptotic expansions to construct the solution of equation (11c) subject to the initial condition (11d) as $K \rightarrow \infty$.

After noting that the initial condition (11d) shows that $\beta \rightarrow 0$ as $\tau \rightarrow 0$, an examination of equation (11c) shows that appropriate scaled variables are, $\hat{\beta} = K\beta_I$, $\hat{\tau} = K\tau$, in terms of which equation (11c) and initial condition (11d) become,

$$\hat{\beta}_{\hat{\tau}} = 1 - \hat{\beta} - K^{-1}\hat{\beta}(\hat{\beta} - \hat{\tau}), \quad \hat{\beta}(0) = 0. \quad (15a, b)$$

We label the region where $\hat{\tau} = O(1)$ as region I and expand $\hat{\beta}(\hat{\tau}; K)$ as

$$\hat{\beta}(\hat{\tau}; K) = \hat{\beta}_0(\hat{\tau}) + K^{-1}\hat{\beta}_1(\hat{\tau}) + o(K^{-1}), \quad \text{as } K \rightarrow \infty, \quad \text{with } \hat{\tau} = O(1). \quad (16)$$

After substituting from (16) into (15a, b), expanding and solving at each order in turn we readily obtain

$$\hat{\beta}_0 = 1 - e^{-\hat{\tau}}, \quad \hat{\beta}_1 = \hat{\tau} - 2 - (\frac{1}{2}\hat{\tau}^2 - 2\hat{\tau} - 1)e^{-\hat{\tau}} + e^{-2\hat{\tau}}. \quad (17)$$

Expansion (16) now shows that, $\hat{\beta} \sim 1 + K^{-1}\hat{\tau} + \dots$ as $K \rightarrow \infty$, for $\hat{\tau} \gg 1$. Thus, expansion (16) becomes non-uniform as $\hat{\tau} \rightarrow \infty$, in particular when $\hat{\tau} = O(K)$ and $\hat{\beta} = O(1)$. To obtain a uniform asymptotic expansion for β_I when $\hat{\tau} = O(K)$ we introduce

region II in which the appropriate variables are τ and $\tilde{\beta} = K\beta_I$. We expand $\tilde{\beta}$ in region II as

$$\tilde{\beta}(\tau; K) = \tilde{\beta}_0(\tau) + K^{-1}\tilde{\beta}_1(\tau) + o(K^{-1}) \quad \text{as } K \rightarrow \infty, \quad \text{with } \tau = O(1). \quad (18)$$

On substituting this expansion into the scaled equation (11c), we immediately obtain the functions $\tilde{\beta}_0$ and $\tilde{\beta}_1$ as, $\tilde{\beta}_0(\tau) = 1/(1-\tau)$, $\tilde{\beta}_1(\tau) = -2/(1-\tau)^3$. After substituting these into expansion (18) we find that this satisfies the appropriate matching conditions with expansion (16) in region I as $\tau \rightarrow 0$. In addition, expansion (18) clearly becomes non-uniform as $\tau \rightarrow 1$, in particular when $\tau = 1 - O(K^{-\frac{1}{2}})$ and $\tilde{\beta} = O(K^{\frac{1}{2}})$. To deal with this non-uniformity we introduce region III, where appropriate scaled variables are $\bar{\beta} = K^{\frac{1}{2}}\beta_I$, $\bar{\tau} = K^{\frac{1}{2}}(\tau - 1)$, and we expand $\bar{\beta}$ as,

$$\bar{\beta}(\bar{\tau}; K) = \bar{\beta}_0(\bar{\tau}) + O(\phi(K)) \quad \text{as } K \rightarrow \infty, \quad \text{with } \bar{\tau} = O(1), \quad (19)$$

and $\phi(K) = o(1)$ as $K \rightarrow \infty$. After substituting expansion (19) into the scaled equation (11c), the leading order problem is readily solved, subject to matching with expansion (18) in region II, to give

$$\bar{\beta}_0(\bar{\tau}) = \bar{\tau} + e^{-\frac{1}{2}\bar{\tau}^2} \int_{-\infty}^{\bar{\tau}} e^{-\frac{1}{2}s^2} ds. \quad (20)$$

By considering the exact solution (12a) we find that $\phi(K) = O(K^{-\frac{1}{2}}e^{-\frac{1}{2}K})$ as $K \rightarrow \infty$ so that the next term in the expansion (19) is exponentially small. Clearly, $\bar{\beta}_0 \sim \bar{\tau}$ as $\bar{\tau} \rightarrow \infty$ and, from the definition of $\bar{\beta}$ and $\bar{\tau}$, a further non-uniformity arises when $\bar{\tau} = O(K^{\frac{1}{2}})$, $\bar{\beta} = O(K^{\frac{1}{2}})$. To deal with this non-uniformity we introduce region IV, where $\beta_I = O(1)$ and $\tau - 1 = O(1)$, and expand β_I as,

$$\beta_I = \beta_0(\tau) + o(1) \quad \text{as } K \rightarrow \infty \quad \text{with } \tau - 1 = O(1). \quad (21)$$

After substituting expansion (21) into equation (11c) we obtain at leading order, after matching to expansion (19) in region III as $\tau \rightarrow 1^+$, $\beta_0 \equiv \tau - 1$. This completes the asymptotic solution of the initial-value problem (11c, d) as $K \rightarrow \infty$. We can summarize the behaviour of β_I and γ_I , from equation (11b), at leading order as

$$\begin{aligned} \text{region I: } \tau = O(K^{-1}), \quad \beta_I \sim K^{-1}(1 - e^{-\tau}), \\ \gamma_I \sim 1 - K^{-1}\hat{\tau} \quad \text{as } K \rightarrow \infty \quad \text{with } \hat{\tau} = K\tau; \end{aligned} \quad (22a)$$

$$\begin{aligned} \text{region II: } O(K^{-1}) < \tau < 1 - O(K^{-\frac{1}{2}}), \quad \beta_I \sim K^{-1}(1 - \tau)^{-1}, \\ \gamma_I \sim 1 - \tau \quad \text{as } K \rightarrow \infty; \end{aligned} \quad (22b)$$

$$\begin{aligned} \text{region III: } |\tau - 1| = O(K^{-\frac{1}{2}}), \quad \beta_I \sim K^{-\frac{1}{2}}\{\bar{\tau} + e^{-\frac{1}{2}\bar{\tau}^2}(\int_{-\infty}^{\bar{\tau}} e^{-\frac{1}{2}s^2} ds)^{-1}\}, \\ \gamma_I \sim K^{-\frac{1}{2}}e^{-\frac{1}{2}\bar{\tau}^2}(\int_{-\infty}^{\bar{\tau}} e^{-\frac{1}{2}s^2} ds)^{-1} \quad \text{as } K \rightarrow \infty \quad \text{with } \bar{\tau} = K^{\frac{1}{2}}(\tau - 1); \end{aligned} \quad (22c)$$

$$\text{region IV: } \tau > 1 + O(K^{-\frac{1}{2}}), \quad \beta_I \sim \tau - 1, \quad \gamma_I = o(K^{-n}) \quad \forall n > 0 \quad \text{as } K \rightarrow \infty. \quad (22d)$$

The solution of the initial-value problem (11c, d) for $K = 1000$ is illustrated in figure 2a. This was obtained by integrating equation (11c) numerically using a fourth-order Runge–Kutta method and clearly displays the asymptotic structure described in (22). Region I is a thin initial transient region where β_I increases to become of $O(K^{-1})$. In region II, β_I remains of $O(K^{-1})$ and increases slowly whilst γ_I decreases linearly. As the solution enters region III, β_I and γ_I are comparable, of $O(K^{-\frac{1}{2}})$. In region III, γ_I becomes exponentially small, whereas β_I starts to increase more rapidly. In region

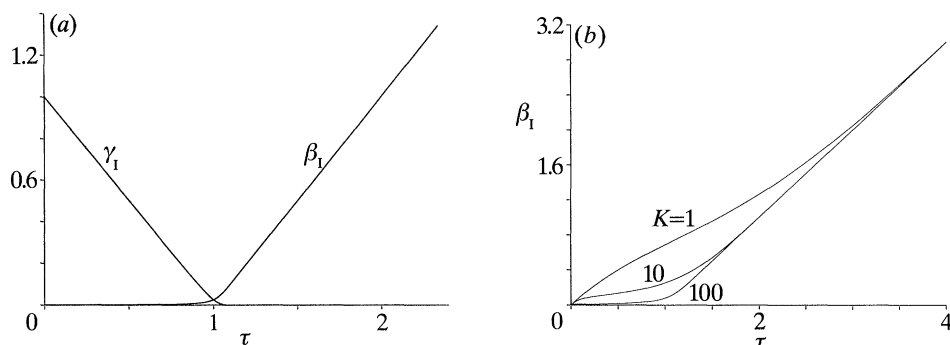


Figure 2. The solution of the initial-value problem (11) for (a) $K = 1000$, (b) $K = 1, 10, 100$.

IV, γ_I remains exponentially small, whereas β_I becomes of $O(1)$ and grows linearly. Figure 2b shows the concentration β_I for various values of K , and indicates that the asymptotic structure (22) develops and becomes more sharply defined as K increases.

We have now constructed the asymptotic solution of the initial-value problem (7b), (9a) for $0 < \epsilon \ll 1$ in an inner region and an outer region and also developed the asymptotic solution of the inner problem (11c, d) for $K \gg 1$ in four asymptotic regions. The solution of the inner problem for $K \gg 1$ has the characteristics of a clock reaction, where B acts as the clock chemical. There is a well-defined induction period in region II which ends in region III when $\tau = \tau_0 = 1 + O(K^{-1/2})$ as $K \rightarrow \infty$.

We can now describe the behaviour of the chemical system (4) when $K \gg 1$ and $\epsilon \ll 1$ (equivalently, $k_1 c_0^2 \gg k_0 p_0$ and $c_0 \ll p_0$, so that step (4b) typically proceeds much faster than step (4a) and the reactant, P, is in large excess over the inhibitor C) in terms of the physical variables b , c and t . After an initial transient period, with duration of $O(1/k_1 c_0)$, the concentration of the clock chemical, B, increases to become of $O(k_0 p_0/k_1 c_0)$. The concentration of B increases very slowly until $t = t_0 \approx c_0/p_0 k_0$. Meanwhile, the concentration of the inhibitor, C, decreases linearly until $t = t_0$, when it becomes small. At $t = t_0$ the concentration of B starts to increase more rapidly and the inhibitor, C, is effectively completely consumed. For $t > t_0$ the concentration of B increases due to the decay of the reactant, P, alone and, $b \rightarrow p_0 - c_0$, as $t \rightarrow \infty$. We note that the end of the induction period, $t_0 = c_0/p_0 k_0$, occurs when the decay of P via step (4a) has produced an amount of B equal to the initial concentration, c_0 , of C, which effectively consumes C completely.

In this section we have identified two chemical mechanisms which can lead to clock reaction behaviour and studied a simple example of each. We will refer to these mechanisms in the following sections as type 1 and type 2.

Type 1. The rate of production of the clock chemical, B, is small when b is small and large when b is large. In addition, b is small initially (§2a).

Type 2. The clock chemical, B, is supplied to the system by some reaction mechanism, for example step (4a), above. In addition, an inhibitor, C, is present initially, and reacts rapidly with B to keep the concentration b small until C is completely consumed, when b can increase (§2b).

We note that in the study of chain reactions the type 2 reaction mechanism is known as inhibition and the corresponding induction period as an inhibition period, whilst the induction period due to a type 1 mechanism is referred to as such (Dainton 1966). However, previous studies of solution phase clock reactions such as those listed in §1 do not distinguish between these two mechanisms.

In the following section we examine a reaction scheme which represents a combination of those which we analysed above, by combining autocatalysis with the action of an inhibitor.

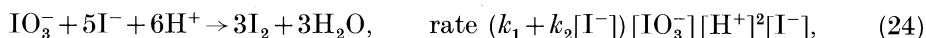
3. Indirect autocatalysis with an inhibitor: the iodate–arsenous-acid reaction

In this section we examine a reaction scheme that consists of two steps which, overall, are autocatalytic in one of the reactants, A. In addition, the second step represents the action of an inhibitor, C, on the clock chemical, B. A simple scheme which is a combination of the two systems that we studied in §2 is,

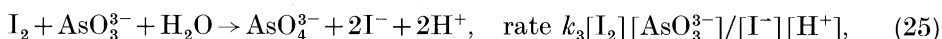


where A is a reactant with concentration a . The system (23a, b) is, however, closely related to a well-known model of the iodate–arsenous-acid reaction and we take this opportunity to present a careful analysis of this model. The iodate–arsenous-acid reaction can be described by two component steps:

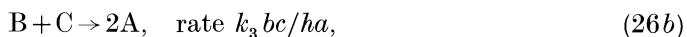
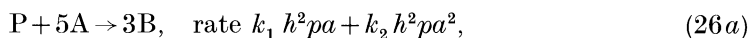
(i) the Dushman reaction (Dushman 1904; Liebavsky & Roe 1979)



(ii) the Roebuck reaction (Roebuck 1902)



where $k_1 \approx 4.5 \times 10^3 \text{ M}^{-3} \text{ s}^{-1}$, $k_2 \approx 4.36 \times 10^8 \text{ M}^{-4} \text{ s}^{-1}$, $k_3 \approx 3.2 \times 10^{-2} \text{ M s}^{-1}$ are reaction rate constants and $[\text{X}]$ is the concentration of the chemical species X. The form of these reaction rate laws and the values of k_1 , k_2 and k_3 are determined experimentally. Experiments on this reaction are often performed in a buffered solution, so that the acidity is constant, and therefore in our analysis we assume that $[\text{H}^+]$ is constant. The basic kinetic model of the reaction is then



where $P \equiv \text{IO}_3^-$, $A \equiv \text{I}^-$, $B \equiv \text{I}_2$, $C \equiv \text{AsO}_3^{3-}$ and $h \equiv [\text{H}^+]$ is a positive constant. A comparison of the two systems (23) and (26) shows that the basic structure of the reaction steps is very similar with A acting as an indirect autocatalyst and C playing the role of the inhibitor. Although the reaction rate laws are different we find that the qualitative behaviour of the two systems (23) and (26) is identical. Finally, we note that this model scheme with $C \equiv \text{HSO}_3^{2-}$ also gives a good description of the kinetics of the iodine–bisulphate clock reaction (Cooke 1979).

The reaction rate equations for the system (26) are

$$\frac{dp}{dt} = -k_1 h^2 pa - k_2 h^2 pa^2, \quad \frac{da}{dt} = -5k_1 h^2 pa - 5k_2 h^2 pa^2 + \frac{2k_3 bc}{ha}, \quad (27a, b)$$

$$\frac{db}{dt} = 3k_1 h^2 pa + 3k_2 h^2 pa^2 - \frac{k_3 bc}{ha}, \quad \frac{dc}{dt} = -\frac{k_3 bc}{ha}. \quad (27c, d)$$

By integrating appropriate linear combinations of equations (27) we find that,

$$p = \frac{1}{3}(c - b - c_0 + 3p_0), \quad a = \frac{1}{3}(-c - 5b + c_0 + 3a_0), \quad (28a, b)$$

where $p = p_0, \quad a = a_0, \quad b = 0, \quad c = c_0 \quad \text{at} \quad t = 0. \quad (29)$

On substituting from (28) into (27c, d) we obtain the reaction rate equations for b and c as,

$$db/dt = h^2(c - b - c_0 + 3p_0) [k_1(-\frac{1}{3}c - \frac{5}{3}b + \frac{1}{3}c_0 + a_0) + k_2(-\frac{1}{3}c - \frac{5}{3}b + \frac{1}{3}c_0 + a_0)^2] - k_3 bc/h(-\frac{1}{3}c - \frac{5}{3}b + \frac{1}{3}c_0 + a_0), \quad (30)$$

$$dc/dt = -k_3 bc/h(-\frac{1}{3}c - \frac{5}{3}b + \frac{1}{3}c_0 + a_0). \quad (31)$$

We now introduce dimensionless variables as, $\pi = p/c_0, \alpha = a/c_0, \beta = b/c_0, \gamma = c/c_0, \tau = k_2 h^2 c_0^2 t$. In terms of these variables, (28)–(31) become

$$\pi = \frac{1}{3}(\gamma - \beta - 1 + 3\lambda), \quad \alpha = \frac{1}{3}(-\gamma - 5\beta + 1 + 3\epsilon), \quad (32a, b)$$

$$d\beta/d\tau = (\gamma - \beta - 1 + 3\lambda) \{ \delta(-\frac{1}{3}\gamma - \frac{5}{3}\beta + \frac{1}{3} + \epsilon) + (-\frac{1}{3}\gamma - \frac{5}{3}\beta + \frac{1}{3} + \epsilon)^2 \} - K\beta\gamma/(-\frac{1}{3}\gamma - \frac{5}{3}\beta + \frac{1}{3} + \epsilon), \quad (32c)$$

$$d\gamma/d\tau = -K\beta\gamma/(-\frac{1}{3}\gamma - \frac{5}{3}\beta + \frac{1}{3} + \epsilon), \quad (32d)$$

$$\pi = \lambda, \quad \alpha = \epsilon, \quad \beta = 0, \quad \gamma = 1 \quad \text{at} \quad \tau = 0, \quad (32e)$$

where the four dimensionless parameters are

$$\lambda = p_0/c_0, \quad \epsilon = a_0/c_0, \quad K = k_3/k_2 h^3 c_0^2, \quad \delta = k_1/k_2 c_0. \quad (33)$$

The parameters λ and ϵ are the dimensionless initial concentrations of the reactants P and A respectively. The parameter K measures the reaction rate of the step (26b) relative to that of the step (26a), whereas δ is a measure of the degree of quadratic autocatalysis relative to cubic autocatalysis in reaction step (26a).

The second-order autonomous system of equations (32c, d) subject to initial conditions (32e) is the full initial-value problem for the time evolution of the concentrations β and γ , and hence, via (32a, b), π and α . To determine the nature of the solution of this initial value problem we first consider the behaviour of solutions of equations (32c, d) in the (β, γ) phase plane. The system (32c, d) has six equilibrium points at $(0, 1 - 3\lambda)$, $(3\lambda - 1, 0)$, $(\frac{1}{5}[3\epsilon + 3\delta + 1], 0)$, $(0, 3\epsilon + 3\delta + 1)$, $(0, 3\epsilon + 1)$ and $(\frac{1}{5}(3\epsilon + 1), 0)$. The point $(0, 1 - 3\lambda)$ has eigenvalues and associated eigenvectors,

$$\mu_1 = -K(1 - 3\lambda)/(\lambda + \epsilon), \quad \mu_2 = -\delta(\lambda + \epsilon) - (\lambda + \epsilon)^2, \quad (34a)$$

$$e_{\mu_1} = (1, 1)^T, \quad e_{\mu_2} = (\mu_2, \mu_1)^T, \quad (34b)$$

and hence is a saddle point for $\lambda > \frac{1}{3}$ and a stable node for $0 \leq \lambda \leq \frac{1}{3}$. The point $(3\lambda - 1, 0)$ has eigenvalues and associated eigenvectors

$$\nu_1 = -\delta(\epsilon + 2 - 5\lambda) - (\epsilon + 2 - 5\lambda)^2, \quad \nu_2 = -K(3\lambda - 1)/(\epsilon + 2 - 5\lambda), \quad (34c)$$

$$e_{\nu_1} = (1, 0)^T, \quad e_{\nu_2} = (1, 1)^T, \quad (34d)$$

and hence is a saddle point for $0 \leq \lambda < \frac{1}{5}$, a stable node for $\frac{1}{3} < \lambda < \frac{1}{5}(\epsilon + 2)$, an unstable node for $\frac{1}{5}(\epsilon + 1) < \lambda < \frac{1}{5}(\epsilon + 2 + \delta)$ and a saddle point for $\lambda > \frac{1}{5}(\epsilon + 2 + \delta)$. The point $(\frac{1}{5}(3\epsilon + 3\delta + 1), 0)$ has eigenvalues and associated eigenvectors

$$\bar{\mu}_1 = K(3\epsilon + 3\delta + 1)/5\delta, \quad \bar{\mu}_2 = \delta(5\lambda - \epsilon - \delta - 2), \quad (35a)$$

$$e_{\bar{\mu}_1} = (\bar{\mu}_2 - \bar{\mu}_1, \frac{1}{5}\bar{\mu}_2)^T, \quad e_{\bar{\mu}_2} = (1, 0)^T, \quad (35b)$$

and hence is a saddle point for $0 < \lambda < \frac{1}{5}(\epsilon + 2 + \delta)$ and an unstable node for $\lambda > \frac{1}{5}(\epsilon + 2 + \delta)$. Finally, the point $(0, 3\epsilon + 3\delta + 1)$ has eigenvalues $\bar{\nu}_1$ and $\bar{\nu}_2$ given by the roots of the quadratic equation

$$\bar{\nu}^2 - a_1 \bar{\nu} - a_2 = 0, \quad (35c)$$

$$\text{where } a_1 = 5\delta(\epsilon + \delta + \lambda) + K(3\epsilon + 3\delta + 1)/\delta, \quad a_2 = K(\epsilon + \delta + \lambda)(3\epsilon + 3\delta + 1). \quad (35d)$$

The associated eigenvectors are

$$\bar{e}_{\nu_1} = (\bar{\nu}_1, K(3\epsilon + 3\delta + 1)/\delta)^T, \quad \bar{e}_{\nu_2} = (\bar{\nu}_2, K(3\epsilon + 3\delta + 1)/\delta)^T. \quad (35e)$$

Since $a_2 > 0$ for $\lambda > 0$, equation (35c) shows that $\bar{\nu}_1 \bar{\nu}_2 < 0$ and hence the equilibrium point $(0, 3\epsilon + 3\delta + 1)$ is a saddle for all $\lambda > 0$. The remaining two equilibrium points are non-simple since they lie on the singular line $\gamma + 5\beta = 3\epsilon + 1$, which we label as L. In the neighbourhood of L, away from the equilibrium points, $\beta_\tau \sim \gamma_\tau$, and hence integral paths meet L with unit gradient. A further consideration of equation (32d) then shows that in the first quadrant of the (β, γ) phase plane integral paths originate singularly at L at finite time, whereas in the second and fourth quadrants integral paths terminate singularly at L at finite time.

To study the behaviour of integral paths in the neighbourhood of the equilibrium point $(0, 1 + 3\epsilon)$ we define new variables,

$$\beta = B, \quad \gamma = 1 + 3\epsilon + C. \quad (36a)$$

After substituting these new variables into equations (32c, d) we find that for $|B|, |C| \ll 1$, at leading order,

$$\frac{dB}{d\tau} = -\delta(\epsilon + \lambda)(5B + C) + \frac{3K(1 + 3\epsilon)B}{(5B + C)}, \quad \frac{dC}{d\tau} = \frac{3K(1 + 3\epsilon)B}{(5B + C)}, \quad (36b, c)$$

These equations admit solutions which pass through the equilibrium point of the form,

$$B = C + o(C), \quad B = \frac{\delta(\epsilon + \lambda)C^2}{3K(1 + 3\epsilon)} + o(C^2) \quad \text{as } C \rightarrow 0. \quad (37a, b)$$

On integral paths of the form (37a) equation (36c) shows that

$$C = \frac{1}{2}K(1 + 3\epsilon)\tau + \text{const.} \quad (38a)$$

whilst on integral paths of the form (37b),

$$C = \text{const. } e^{\delta(\epsilon + \lambda)\tau}. \quad (38b)$$

Equation (38a) shows that $B = 0, C = 0$ is not an equilibrium point in terms of the dynamics on paths of the form (37a). However, on paths of the form (37b), $B \rightarrow 0$ and $C \rightarrow 0$ as $\tau \rightarrow -\infty$. The phase portrait of the system of equations (36b, c) is sketched in figure 3 in the (B, C) phase plane. To determine the behaviour of the integral paths in the neighbourhood of the equilibrium point $(\frac{1}{5}(1 + 3\epsilon), 0)$ we define new variables as

$$\beta = \frac{1}{5}(1 + 3\epsilon) + \bar{B}, \quad \gamma = \bar{C}. \quad (39a)$$

At leading order for $|\bar{B}|, |\bar{C}| \ll 1$, equations (32c, d) become

$$\frac{d\bar{B}}{d\tau} = \frac{1}{5}\delta(\epsilon + 2 - 5\lambda)(5\bar{B} + \bar{C}) + \frac{3K(1 + 3\epsilon)\bar{C}}{5(5\bar{B} + \bar{C})}, \quad \frac{d\bar{C}}{d\tau} = \frac{3K(1 + 3\epsilon)\bar{C}}{5(5\bar{B} + \bar{C})}. \quad (39b, c)$$

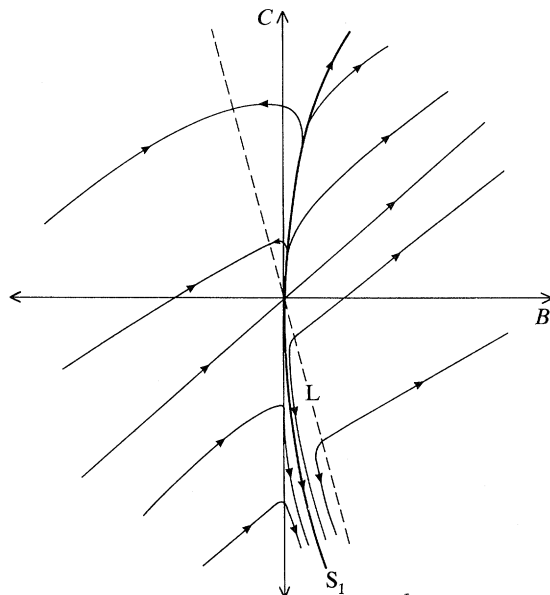


Figure 3. A sketch of the phase portrait of the system of equations (36*b, c*) in the (*B, C*) phase plane.

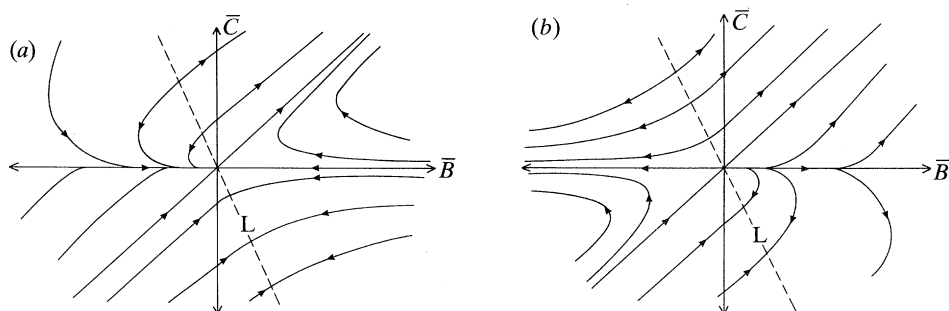


Figure 4. A sketch of the phase portrait of the system of equations (39*b, c*) in the (\bar{B}, \bar{C}) phase plane for: (a) $\lambda > \frac{1}{5}(\epsilon + 2)$, (b) $0 < \lambda < \frac{1}{5}(\epsilon + 2)$.

These equations have the exact solution,

$$\bar{B} = \text{const. } e^{\delta(\epsilon+2-5\lambda)\tau}, \quad \bar{C} = 0, \quad (40a)$$

and also a solution of the form,

$$\bar{B} = \bar{C} + o(1), \quad \bar{C} = \frac{1}{2}K(1 + 3\epsilon)\tau + \text{const.}, \quad \text{as } \bar{C} \rightarrow 0. \quad (40b)$$

The point $\bar{B} = \bar{C} = 0$ is therefore not an equilibrium point in terms of the dynamics on paths of the form (40*b*). However, on the integral path (40*a*), $\bar{B} \rightarrow 0, \bar{C} \rightarrow 0$ as $\tau \rightarrow \infty$ for $\lambda > \frac{1}{5}(\epsilon + 2)$, whereas $\bar{B} \rightarrow 0, \bar{C} \rightarrow 0$ as $\tau \rightarrow -\infty$ for $0 \leq \lambda < \frac{1}{5}(\epsilon + 2)$. The phase portrait of the system of equations (39*b, c*) is sketched in figure 4*a* for $\lambda > \frac{1}{5}(\epsilon + 2)$ and in figure 4*b* for $0 \leq \lambda < \frac{1}{5}(\epsilon + 2)$, in the (\bar{B}, \bar{C}) phase plane. Finally, we note that the system of equations (32*c, d*) has two integral paths which are straight lines, namely, $\gamma = 0$ and $\gamma = \beta + 1 - 3\lambda$.

We now turn our attention to the solution of the initial value problem (32*c-e*). Since we have enough information to sketch the phase portrait of the system of

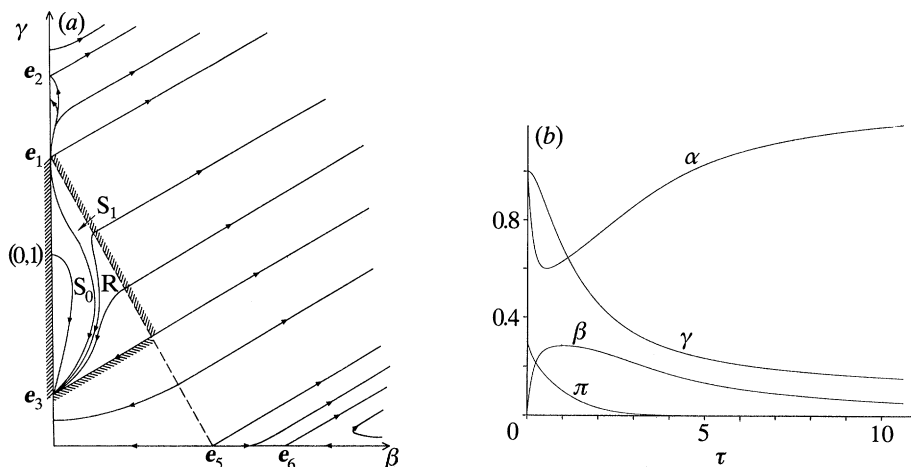


Figure 5. (a) A sketch of the phase portrait of the system of equations (32c, d) in the (β, γ) phase plane for $0 < \lambda < \frac{1}{3}$. The equilibrium points are labelled as $e_1 = (0, 3\epsilon + 1)$, $e_2 = (0, 3\epsilon + 3\delta + 1)$, $e_3 = (0, 1 - 3\lambda)$, $e_4 = (3\lambda - 1, 0)$, $e_5 = (\frac{1}{5}(3\epsilon + 1), 0)$ and $e_6 = (\frac{1}{5}(3\epsilon + 3\delta + 1), 0)$. (b) The solution of the initial value problem (32) for $\lambda = 0.3$, $\epsilon = 1$, $\delta = 1$, $K = 1$.

equations (32c, d) for all $\epsilon, \lambda, \delta > 0$ we can determine the behaviour of the integral path with $\beta = 0, \gamma = 1$ at $\tau = 0$ (which we label as S_0) that represents the solution of the initial-value problem. We find that there are three cases to consider.

(i) $0 < \lambda \leq \frac{1}{3}$

The equilibrium point $(0, 1 - 3\lambda)$ is a stable node, whereas the equilibrium point $(3\lambda - 1, 0)$ is a saddle point and lies outside the first quadrant of the (β, γ) phase plane, which is sketched in figure 5a. Now consider the region R , defined by

$$R = \{(\beta, \gamma) : \beta, \gamma \geq 0, 1 + 3\epsilon - 5\beta \geq \gamma \geq \beta + 1 - 3\lambda\}. \quad (41)$$

Equations (32c, d) show that no integral path is directed out of the boundary of the region R . Therefore, via the Poincaré–Bendixson theorem, all integral paths that enter R must be asymptotic to the equilibrium point $(0, 1 - 3\lambda)$ as $\tau \rightarrow \infty$, since this is the only stable equilibrium point which lies within R . In particular, the integral path S_0 , which represents the solution of the initial-value problem (32c–e), is asymptotic to the equilibrium point $(0, 1 - 3\lambda)$ since it enters the region R at $\tau = 0$. Therefore,

$$\pi \rightarrow 0, \quad \alpha \rightarrow \lambda + \epsilon, \quad \beta \rightarrow 0, \quad \lambda \rightarrow 1 - 3\lambda \quad \text{as } \tau \rightarrow \infty. \quad (42)$$

A typical solution is illustrated in figure 5b for the case $\lambda = 0.3, \epsilon = 1, \delta = 1, K = 1$. This was obtained by integrating equations (32c, d) numerically using a fourth order Runge–Kutta method. In Hanna *et al.* (1982) this is referred to as the case of excess arsenous acid. The reaction is effectively just the autocatalytic conversion of $P \equiv \text{IO}_3^-$ to $A \equiv \text{I}^-$, and $C \equiv \text{AsO}_3^{3-}$ is not completely consumed.

(ii) $\frac{1}{3} < \lambda \leq \frac{1}{5}(\epsilon + 2)$

The equilibrium point $(0, 1 - 3\lambda)$ is a saddle point and lies outside the first quadrant of the (β, γ) phase plane, whereas the equilibrium point $(3\lambda - 1, 0)$ is now a stable node and lies within the first quadrant, which is illustrated in figure 6a. By the

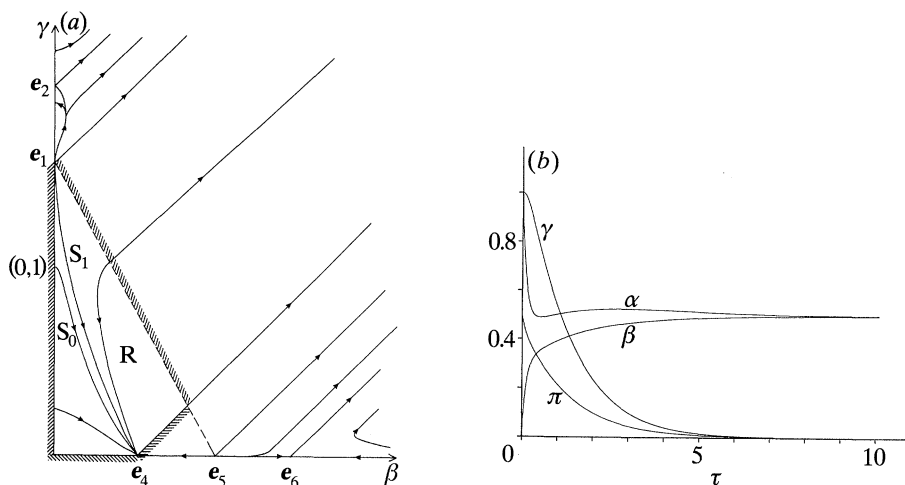


Figure 6. (a) A sketch of the phase portrait of the system of equations (32c, d) in the (β, γ) phase plane for $\frac{1}{3} < \lambda < \frac{1}{5}(\epsilon + 2)$. The labels e_1 – e_6 are defined in the caption for figure 5. (b) The solution of the initial-value problem (32) for $\lambda = 0.5$, $\epsilon = 1$, $\delta = 1$, $K = 1$.

argument given above, the integral path S_0 , which represents the solution of the initial-value problem (32c–e) is asymptotic to the only stable equilibrium point which lies within the region R which in this case is the point $(3\lambda - 1, 0)$. Therefore,

$$\pi \rightarrow 0, \quad \alpha \rightarrow 2 + \epsilon - 5\lambda, \quad \beta \rightarrow 3\lambda - 1, \quad \gamma \rightarrow 0 \quad \text{as } \tau \rightarrow \infty. \quad (43)$$

A typical solution is illustrated in figure 6b for the case $\lambda = 0.5$, $\epsilon = 1$, $\delta = 1$, $K = 1$. In Hanna *et al.* (1982) this is referred to as the case of excess iodate, along with case (iii) below. In this case there is a sufficient concentration of $P \equiv \text{IO}_3^-$ present initially to produce enough $B = \text{I}_2$ to consume all of the inhibitor, $C \equiv \text{AsO}_3^{2-}$, but not enough P to completely consume all of the reactant $A \equiv \text{I}^-$.

(iii) $\lambda > \frac{1}{5}(\epsilon + 2)$

The equilibrium point $(0, 1 - 3\lambda)$ is a saddle point and lies outside the first quadrant of the (β, γ) phase plane. The equilibrium points $(3\lambda - 1, 0)$ and $(\frac{1}{5}(3\epsilon + 3\delta + 1), 0)$ are coincident when $\lambda = \frac{1}{5}(\epsilon + 2 + \delta)$ and undergo an exchange of stability via a saddle-node bifurcation. However, these points do not affect the behaviour of the integral path S_0 , since they lie outside the region R . The (β, γ) phase plane is sketched in figure 7a for $\lambda > \frac{1}{5}(\epsilon + 2 + \delta)$. By the argument given above, the integral path S_0 is now asymptotic to the point $(\frac{1}{5}(1 + 3\epsilon), 0)$ as $\tau \rightarrow \infty$. Therefore,

$$\pi \rightarrow \frac{1}{5}(5\lambda - 2 - \epsilon), \quad \alpha \rightarrow 0, \quad \beta \rightarrow \frac{1}{5}(1 + 3\epsilon), \quad \gamma \rightarrow 0, \quad \text{as } \tau \rightarrow \infty. \quad (44)$$

A typical solution is illustrated in figure 7b for the case $\lambda = 0.8$, $\epsilon = 1$, $\delta = 1$, $K = 1$. In this case there is a sufficient concentration of $P = \text{IO}_3^-$ present to produce enough $B = \text{I}_2$ to consume all of the inhibitor, $C \equiv \text{AsO}_3^{2-}$ and then all of the reactant, $A \equiv \text{I}^-$.

These three cases are in good agreement with experimental observations of the behaviour of the iodate–arsenous–acid reaction, as described by Hanna *et al.* (1982). The indicator that is generally added to the reaction mixture is starch. This leads to a colour change from a clear solution to a black solution in the presence of a

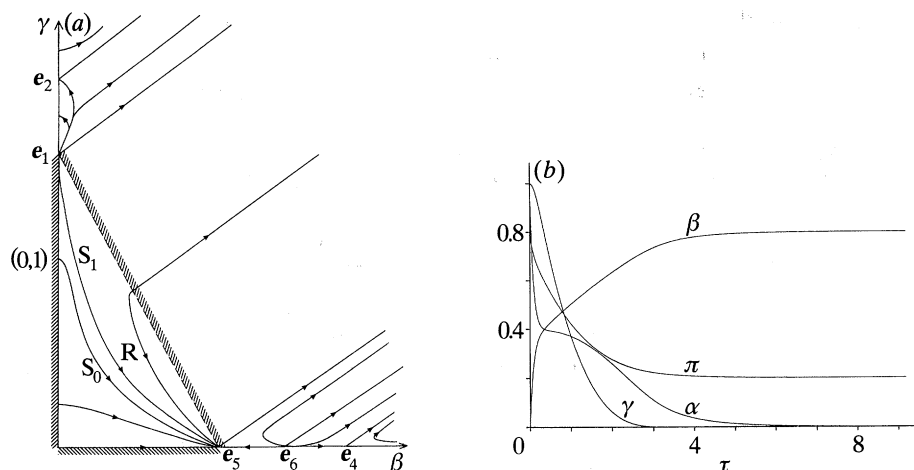


Figure 7. (a) A sketch of the phase portrait of the system of equations (32c, d) in the (β, γ) phase plane for $\lambda > \frac{1}{5}(\epsilon + 2)$. The labels e_1 – e_6 are defined in the caption of figure 5. (b) The solution of the initial-value problem (32) for $\lambda = 0.8$, $\epsilon = 1$, $\delta = 1$, $K = 1$.

significant concentration of the clock chemical, iodine, which is represented by B in the reaction scheme (26). In case (i) the concentration, β , of iodine reaches a maximum and then decays to zero as $\tau \rightarrow \infty$. The reaction mixture therefore becomes black for a short period and then becomes clear again. In case (ii) and (iii) $\beta \rightarrow \text{constant}$ as $\tau \rightarrow \infty$, which results in a permanently black reaction mixture. Either of these types of colour change can occur after a significant induction period. The iodate–arsenous-acid reaction can, therefore, behave as a clock reaction and we now turn our attention to the possibility of this type of behaviour in the solution of the initial-value problem (32c–e).

As a preliminary, we consider the dimensionless parameters given in (33). In the typical experiments outlined in Hanna *et al.* (1982) $a_0 \approx 10^{-5}$ M, $c_0 \approx 10^{-2}$ M, $p_0 \approx 10^{-3}$ M and h ranges between 8×10^{-4} M and 1.3×10^{-2} M. Combined with the values for k_1, k_2 and k_3 given earlier this leads to $\epsilon \approx 10^{-3}$, $\delta \approx 10^{-3}$ and $\lambda \approx 1$. The parameter K is very sensitive to changes in $h = [\text{H}^+]$ and decreases from approximately 1000 to 1 as h increases from 10^{-3} M to 10^{-2} M. Clearly in these experiments $0 < \epsilon \ll 1$ with $\delta = O(\epsilon)$ and, for sufficiently low values of h (low acidity) $K \gg 1$. We now show that when $\epsilon \ll 1$ and $K = O(1)$ clock reaction behaviour occurs due to the type 1 mechanism, whereas for $\epsilon = O(1)$ and $K \gg 1$ clock reaction behaviour arises due to the type 2 mechanism. We also find that when $\epsilon \ll 1$ and $K \gg 1$ the type 1 mechanism is dominant during the long induction period.

(a) *Asymptotic solution of the initial-value problem for $0 < \epsilon \ll 1$ with $\delta = O(\epsilon)$ and $K = O(1)$*

Here we examine the initial-value problem (32c–e) when $\epsilon \ll 1$ with $\delta = O(\epsilon)$ and $K = O(1)$, which is in line with the parameter values appropriate for the experiments of Hanna *et al.* (1982), and we may expect clock like behaviour of type 1. We define the constant, Δ , by $\delta = \Delta\epsilon$, with $\Delta = O(1)$ as $\epsilon \rightarrow 0$, and develop an asymptotic solution of the initial-value problem (32) for $0 < \epsilon \ll 1$. We find that there is an induction period during which the concentration β remains small, of $O(\epsilon^3)$. The solution during the induction period develops in two asymptotic regions, which we

label as region I and region II. Appropriate scaled variables for region I are, $\beta = \epsilon^3 \hat{\beta}$, $\gamma = 1 + \epsilon^3 \hat{\gamma}$, $\tau = \epsilon \hat{\tau}$, and we expand $\hat{\beta}$ and $\hat{\gamma}$ as

$$\hat{\beta} = \hat{\beta}_0 + \epsilon^2 \hat{\beta}_1 + o(\epsilon^2), \quad \hat{\gamma} = \hat{\gamma}_0 + \epsilon^2 \hat{\gamma}_1 + o(\epsilon^2) \quad \text{as } \epsilon \rightarrow 0, \quad \text{with } \hat{\tau} = O(1). \quad (45a)$$

After writing equations (32c, d) in terms of the above scaled variables, substituting expansions (45a) for $\hat{\beta}$ and $\hat{\gamma}$ and solving the resulting equations for $\hat{\beta}_0, \hat{\beta}_1, \hat{\gamma}_0$ and $\hat{\gamma}_1$, we obtain

$$\hat{\beta}_0 = \frac{3\lambda(\Delta+1)}{K}(1 - e^{-K\hat{\tau}}), \quad \hat{\gamma}_0 = \frac{3\lambda(\Delta+1)}{K}(1 - e^{-K\hat{\tau}} - K\hat{\tau}), \quad (45b)$$

as the solutions which satisfy the initial conditions given by (32e). For brevity, the expressions for $\hat{\beta}_1$ and $\hat{\gamma}_1$ are not presented, but given in Billingham (1991). Expansions (45a) now show that

$$\left. \begin{aligned} \hat{\beta} &\sim \frac{3\lambda(\Delta+1)}{K} + \epsilon^2 \frac{3\lambda^2(\Delta+1)(2\Delta+3)\hat{\tau}}{K} + o(\epsilon^2), \\ \hat{\gamma} &\sim -3\lambda(\Delta+1)\hat{\tau} - \epsilon^2 \frac{3}{2}\lambda^2(\Delta+1)(\Delta+2)\hat{\tau}^2 + o(\epsilon^2), \end{aligned} \right\} \quad (45c)$$

as $\epsilon \rightarrow 0$, for $\hat{\tau} \gg 1$. These approximations become non-uniform as $\hat{\tau} \rightarrow \infty$, in particular when $\hat{\tau} = O(\epsilon^{-2})$, $\hat{\beta} = O(1)$ and $\hat{\gamma} = O(\epsilon^{-2})$, and the solution enters region II. Appropriate scaled variables in region II are, $\beta = \epsilon^3 \tilde{\beta}$, $\gamma = 1 + \epsilon \tilde{\gamma}$, $\tau = \epsilon^{-1} \tilde{\tau}$, and we expand $\tilde{\beta}$ and $\tilde{\gamma}$ as

$$\tilde{\beta} = \tilde{\beta}_0 + o(1), \quad \tilde{\gamma} = \tilde{\gamma}_0 + o(1) \quad \text{as } \epsilon \rightarrow 0, \quad \text{with } \tilde{\tau} = O(1). \quad (46a)$$

After writing equations (32c, d) in terms of the above scaled variables and solving the leading order equations, we obtain the solutions

$$\hat{\beta}_0 = \frac{3\lambda\Delta^3(\Delta+1)e^{2\lambda\Delta\tilde{\tau}}}{K(\Delta+1 - e^{\lambda\Delta\tilde{\tau}})^3}, \quad \hat{\gamma}_0 = \frac{3(\Delta+1)(1 - e^{\lambda\Delta\tilde{\tau}})}{(\Delta+1 - e^{\lambda\Delta\tilde{\tau}})}, \quad (46b)$$

which match with expansions (45a) in region I as $\tilde{\tau} \rightarrow 0$. This approximation clearly becomes non-uniform as $\tilde{\tau} \rightarrow \tilde{\tau}_0$, where

$$\tilde{\tau}_0 = [\ln(\Delta+1)]/\Delta\lambda, \quad (46c)$$

in particular, when $\tilde{\tau} = \tilde{\tau}_0 - O(\epsilon)$, $\hat{\beta} = O(\epsilon^{-3})$, $\hat{\gamma} = O(\epsilon^{-1})$. To complete the solution, we introduce a final asymptotic region, which we label as region III, where $\beta = \beta_0 + o(1)$, $\gamma = \gamma_0 + o(1)$, as $\epsilon \rightarrow 0$ with $T = O(1)$, and $\tau = \epsilon^{-1}\tilde{\tau}_0 + T$. In terms of these variables, equations (32c, d) become, at leading order,

$$\frac{d\beta_0}{dT} = (\gamma_0 - \beta_0 - 1 + 3\lambda) \left(-\frac{1}{3}\gamma_0 - \frac{5}{3}\beta_0 + \frac{1}{3}\right)^2 - \frac{K\beta_0\gamma_0}{\left(-\frac{1}{3}\gamma_0 - \frac{5}{3}\beta_0 + \frac{1}{3}\right)}, \quad (47a)$$

$$\frac{d\gamma_0}{dT} = -\frac{K\beta_0\gamma_0}{\left(-\frac{1}{3}\gamma_0 - \frac{5}{3}\beta_0 + \frac{1}{3}\right)}, \quad (47b)$$

which are to be solved subject to the matching condition,

$$\beta_0 \rightarrow 0, \quad \gamma_0 \rightarrow 1 \quad \text{as } T \rightarrow -\infty. \quad (47c)$$

Equations (47a, b) are equivalent to equations (32c, d) with $\delta = \epsilon = 0$. For $\delta > 0$, $\epsilon > 0$ there is a unique solution of equations (32c, d) that satisfies $\beta \rightarrow 0$, $\gamma \rightarrow 1 + 3\epsilon$ as $\tau \rightarrow -\infty$, with $\beta > 0$, $\gamma < 1$, which we have labelled as S_1 in figures 3, 5a, 6a, and

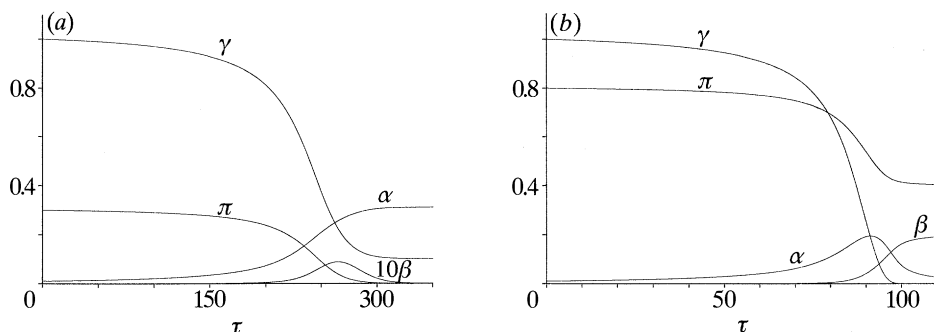


Figure 8. The solution of the initial-value problem (32) for $\epsilon = 0.01$, $\delta = 0.01$, $K = 1$ and (a) $\lambda = 0.3$, (b) $\lambda = 0.8$.

7a. It is readily shown that this is also the case when $\delta = \epsilon = 0$, and hence the boundary-value problem (47a-c) has a unique solution. We also note that the phase portrait of the system of equations (32c, d) in the (β, γ) phase plane within the region R , defined by (41), is qualitatively similar to the phase portrait of the system (47a, b) in the (β_0, γ_0) phase plane within the region R_0 , where R_0 is equivalent to R with $\beta = \beta_0$, $\gamma = \gamma_0$ and $\epsilon = 0$. There are, therefore, three cases to consider.

$$\left. \begin{array}{l} \text{(i)} \quad 0 < \lambda \leq \frac{1}{3}: \beta_0 \rightarrow 0, \quad \gamma_0 \rightarrow 1 - 3\lambda \quad \text{as } T \rightarrow \infty, \\ \text{(ii)} \quad \frac{1}{3} < \lambda \leq \frac{2}{5}: \beta_0 \rightarrow 3\lambda - 1, \quad \gamma_0 \rightarrow 0 \quad \text{as } T \rightarrow \infty, \\ \text{(iii)} \quad \lambda > \frac{2}{5}: \beta_0 \rightarrow \frac{1}{5}, \quad \gamma_0 \rightarrow 0 \quad \text{as } T \rightarrow \infty. \end{array} \right\} \quad (48)$$

These cases are equivalent to those described above for the full initial-value problem (32c-e), and the asymptotic solution for $0 < \epsilon \ll 1$, $\delta = O(\epsilon)$ is therefore complete.

Region I is a thin initial transient region where β becomes of $O(\epsilon^3)$ and in the (β, γ) phase plane the solution is asymptotic to the integral path S_1 in the neighbourhood of the equilibrium point $(0, 1 + 3\epsilon)$. Region II represents a long induction period during which the solution at leading order is given by the integral path S_1 in the neighbourhood of the point $(0, 1 + 3\epsilon)$ with $\beta = O(\epsilon^3)$ and $1 + 3\epsilon - \gamma = O(\epsilon)$. The induction period ends when $\tau = \epsilon^{-1}\bar{\tau}_0 + O(1)$ and the solution enters region III. The solution in region III is obtained from the full equations (32c, d) with $\epsilon = \delta = 0$, and is represented by the integral path S_1 at leading order. The behaviour of β and γ as $\tau \rightarrow \infty$ depends upon the value of λ as described by (48), which is in agreement with results (42), (43), (44) for the solution of the full initial value (32c-e) with $\epsilon = O(1)$. The solution of the initial value problem for $\epsilon = 0.01$, $\delta = 0.01$, $K = 1$ is shown in figure 8a, b, for $\lambda = 0.3$ (case (i)) and $\lambda = 0.8$ (case (iii)) respectively. We have chosen $\epsilon = \delta = 10^{-2}$ for ease of presentation since, although the induction period is ten times longer for the more realistic values $\epsilon = \delta = 10^{-3}$, the qualitative form of the solution is the same. The time $\tau_0 = \epsilon^{-1}\bar{\tau}_0 \approx 231$ and 87 for $\lambda = 0.3$ and $\lambda = 0.8$ respectively, is in good agreement with the form of the numerical solution in each case. In terms of the physical variables, we find that t_0 , the duration of the induction period is given by,

$$t_0 \approx \frac{\ln [1 + k_1/k_2 a_0]}{k_1 p_0 h^2} \quad \text{for } a_0 \ll c_0 \quad \text{and} \quad k_1 \ll k_2 c_0. \quad (49)$$

This expression leads to induction times ranging from a few seconds to a few days, in good agreement with experimental observations. Since t_0 is very sensitive to

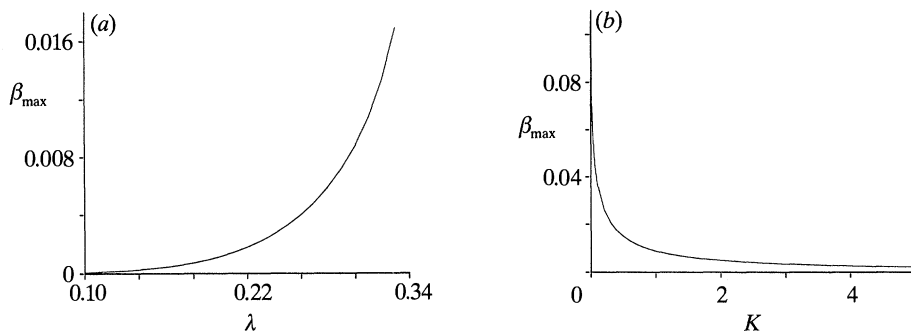


Figure 9. Graphs of the function $\beta_{\max}(\lambda, K)$ when $\epsilon = \delta = 0.01$: (a) for $K = 1$ plotted against λ , (b) for $\lambda = 0.3$ plotted against K .

changes in h , the acidity of the reaction mixture, expression (49) explains why a slight mismeasurement of the pH can be unfortunate when the iodate–arsenous-acid reaction is used in a lecture demonstration and $t_0 > 60$ min.

Finally, we note that in case (i), $0 < \lambda \leq \frac{1}{3}$, the concentration β reaches a maximum value, β_{\max} , before decaying to zero as $\tau \rightarrow \infty$. We have shown above that the integral path, S_0 , which represents the solution in the (β, γ) phase plane, lies within the region R , defined by (41). Therefore, $0 \leq \beta_{\max} \leq \frac{1}{2}(\lambda + \epsilon)$ and hence $0 \leq \beta_{\max} \ll 1$ when $0 \leq \lambda \ll 1$, and $0 \leq \epsilon \ll 1$. A graph of β_{\max} against λ for $\epsilon = \delta = 0.01$, $K = 1$ is illustrated in figure 9a. We find that, although $\beta_{\max} = O(1)$ as $\epsilon \rightarrow 0$, since the value of ϵ does not affect the behaviour of S_0 at leading order away from the equilibrium point $(0, 1 + 3\epsilon)$, the numerical value of β_{\max} is small. This is due to the geometry of the phase portrait of the system (32c, d) alone. Figure 9b shows a graph of β_{\max} against K for $\epsilon = \delta = 0.01$, $\lambda = 0.3$. As $K \rightarrow \infty$, $\beta_{\max} \rightarrow 0$, and we show later that $\beta_{\max} = O(K^{-1})$ as $K \rightarrow \infty$. Our numerical results also suggest that $\beta_{\max} \rightarrow \frac{1}{2}(\lambda + \epsilon)$ as $K \rightarrow 0$, a result which is readily obtained from an analysis of the initial-value problem (32c–e) for $0 < K \ll 1$, the details of which are omitted here. Thus, β_{\max} is numerically small unless K is sufficiently small and λ is sufficiently large. The model therefore implies that for the iodate–arsenous-acid reaction in the presence of starch, in the case of excess arsenous acid, (case (i)) the local maximum in the concentration of iodine will not lead to a perceptible colour change of the reaction mixture unless $k_3/k_2 h^3 c_0^2$ and $\frac{1}{3}c_0 - p_0$ are sufficiently small.

(b) *Asymptotic solution of the initial-value problem for $K \gg 1$ with $\epsilon, \delta = O(1)$*

We now consider the solution of the initial-value problem (32c–e) when $K \gg 1$ and $\epsilon, \delta = O(1)$. In this situation we expect clock-like behaviour of type 2. The asymptotic solution of (32c–e) as $K \rightarrow \infty$ is readily obtained and consists of four asymptotic regions. We give the details of the solution in each region at leading order.

Region I: $\hat{\tau} = K\tau = O(1)$, $\beta = K^{-1}\hat{\beta}(\hat{\tau}) + o(K^{-1})$,
 $\gamma = 1 + K^{-1}\hat{\gamma}(\hat{\tau}) + o(K^{-1})$ as $K \rightarrow \infty$,

where

$$\hat{\beta} = 3\epsilon^2\lambda(\delta + \epsilon)(1 - e^{-\hat{\tau}/\epsilon}), \quad \hat{\gamma} = -3\epsilon\lambda(\delta + \epsilon)(\hat{\tau} + \epsilon e^{-\hat{\tau}/\epsilon} - \epsilon). \quad (50), (51)$$

Region II: $O(K^{-1}) < \tau < \tau_0 - O(K^{-\frac{1}{2}})$, $\beta = K^{-1}\tilde{\beta}(\tau) + o(K^{-1})$,
 $\gamma = \tilde{\gamma}(\tau) + o(K^{-1})$ as $K \rightarrow \infty$,

where τ_0 is a constant to be determined and

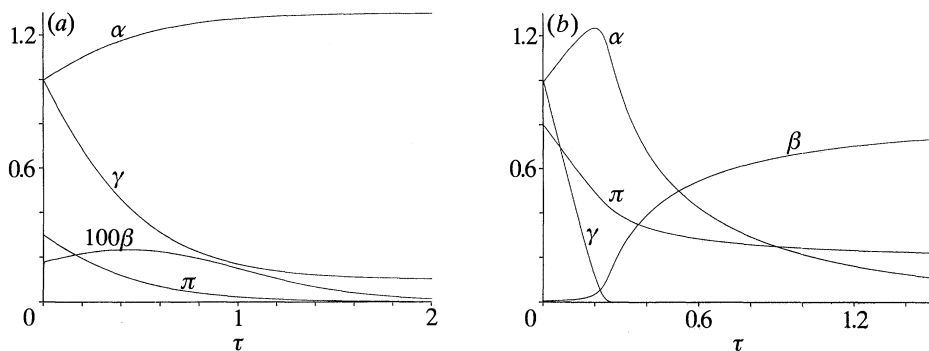


Figure 10. The solution of the initial-value problem (32) for $\epsilon = 1$, $\delta = 1$, $K = 1000$ and: (a) $\lambda = 0.3$, (b) $\lambda = 0.8$.

$$0 = (\tilde{\gamma} - 1 + 3\lambda) \left(\delta - \frac{1}{3}\tilde{\gamma} - \frac{1}{3} + \epsilon \right) \left(-\frac{1}{3}\tilde{\gamma} + \frac{1}{3} + \epsilon \right) - \frac{\tilde{\beta}\tilde{\gamma}}{\left(-\frac{1}{3}\tilde{\gamma} + \frac{1}{3} + \epsilon \right)}, \quad (52a)$$

$$\tilde{\gamma}_\tau = -\tilde{\beta}\tilde{\gamma} / \left(-\frac{1}{3}\tilde{\gamma} + \frac{1}{3} + \epsilon \right), \quad (52b)$$

subject to matching with the solution in region I as $\tau \rightarrow 0$, which gives

$$\tilde{\beta} \rightarrow 3\epsilon^2\lambda(\delta + \epsilon), \quad \tilde{\gamma} \rightarrow 1 \quad \text{as } \tau \rightarrow 0. \quad (52c)$$

Equation (52a) gives

$$\tilde{\beta} = -\frac{1}{27}\tilde{\gamma}^{-1}(\tilde{\gamma} - \tilde{\gamma}_1)(\tilde{\gamma} - \tilde{\gamma}_2)(\tilde{\gamma} - \tilde{\gamma}_3), \quad (53a)$$

where $\tilde{\gamma}_1 = 1 - 3\lambda$, $\tilde{\gamma}_2 = 1 + 3\epsilon$, $\tilde{\gamma}_3 = 1 + 3\epsilon + 3\delta$. On substituting for $\tilde{\beta}$ from (53a) into equation (52b) we obtain,

$$d\tilde{\gamma}/d\tau = -\frac{1}{9}(\tilde{\gamma} - \tilde{\gamma}_1)(\tilde{\gamma} - \tilde{\gamma}_2)(\tilde{\gamma} - \tilde{\gamma}_3), \quad (53b)$$

which is to be solved subject to the matching condition, $\tilde{\gamma}(0) = 1$. The appropriate solution of (53b) is readily obtained in implicit form (Billingham 1991). However, the behaviour of $\tilde{\gamma}$ is most easily studied by examining the form of equation (53b). There are two possibilities.

(i) $0 < \lambda \leq \frac{1}{3}$

In this case, $\tilde{\gamma}$ is monotone decreasing in τ , with $\tilde{\gamma} \rightarrow 1 - 3\lambda$ as $\tau \rightarrow \infty$, and hence, from equations (53a) $\tilde{\beta} \rightarrow 0$ as $\tau \rightarrow \infty$. The approximation in region II remains uniform in K as $\tau \rightarrow \infty$ and no further regions are required. (Formally, $\tau_0 \equiv \infty$ in this case.) This behaviour as $\tau \rightarrow \infty$ is in agreement with that described in case (i) above for the full initial value problem. In this case, region I is a thin initial transient region where β becomes of $O(K^{-1})$. In region II β remains uniformly small of $O(K^{-1})$, whereas γ decreases and $\beta \rightarrow 0$, $\gamma \rightarrow 1 - 3\lambda$ as $\tau \rightarrow \infty$. Clearly, no clock reaction behaviour arises when $0 < \lambda \leq \frac{1}{3}$, $K \gg 1$ and $\epsilon, \delta = O(1)$. The numerical solution of the initial-value problem (32c-e) is illustrated in figure 10a when $\lambda = 0.3$, $K = 1000$, $\epsilon = \delta = 1$, and shows that β remains small for all $\tau \geq 0$.

(ii) $\lambda > \frac{1}{3}$

Equation (53b) again shows that $\tilde{\gamma}$ is monotone decreasing in τ . However, $\tilde{\gamma}(\tau) \rightarrow 0$ as $\tau \rightarrow \tau_0$, where (53b) shows that

$$\tau_0 = \frac{\ln [3 + 1/\epsilon]}{\delta(\epsilon + \lambda)} - \frac{\ln [3 + 1/(\epsilon + \delta)]}{\delta(\epsilon + \lambda + \delta)} - \frac{\ln [3 - 1/\lambda]}{(\epsilon + \lambda)(\epsilon + \lambda + \delta)}. \quad (54)$$

This leads to $\bar{\beta} \rightarrow \infty$ as $\tau \rightarrow \tau_0$, and we conclude that the expansions in region II become non-uniform as $\tau \rightarrow \tau_0$. This non-uniformity corresponds to the end of the induction phase and we note that τ_0 is in agreement with (46c) when $0 < \epsilon \leq 1$ and $\delta = O(\epsilon)$. To continue the development of the solution, we require a further region.

Region III: $\bar{\tau} = K^{\frac{1}{2}}(\tau - \tau_0) = O(1)$, $\beta = K^{-\frac{1}{2}}\bar{\beta} + o(K^{-\frac{1}{2}})$,
 $\gamma = K^{-\frac{1}{2}}\bar{\gamma} + o(K^{-\frac{1}{2}})$ as $K \rightarrow \infty$,

where

$$\bar{\beta}_{\bar{\tau}} = (3\lambda - 1) \left(\epsilon + \frac{1}{3}\right) \left(\epsilon + \frac{1}{3} + \delta\right) - \frac{\bar{\beta}\bar{\gamma}}{\left(\epsilon + \frac{1}{3}\right)}, \quad \bar{\gamma}_{\bar{\tau}} = -\frac{\bar{\beta}\bar{\gamma}}{\left(\epsilon + \frac{1}{3}\right)}, \quad (55a, b)$$

subject to matching with the solution in region II as $\bar{\tau} \rightarrow -\infty$, which gives,

$$\bar{\beta} \sim \left(\epsilon + \frac{1}{3}\right)/\bar{\tau}, \quad \bar{\gamma} \sim -(3\lambda - 1) \left(\epsilon + \frac{1}{3}\right) \left(\epsilon + \frac{1}{3} + \delta\right) \bar{\tau}, \quad \text{as } \bar{\tau} \rightarrow -\infty. \quad (55c)$$

The solution of (55a-c) is determined in Billingham (1991) as,

$$\bar{\beta} = (3\lambda - 1) \left(\epsilon + \frac{1}{3}\right) \left(\epsilon + \frac{1}{3} + \delta\right) \bar{\tau} + \frac{\left(\epsilon + \frac{1}{3}\right) \exp\left[-\frac{1}{2}(3\lambda - 1) \left(\epsilon + \frac{1}{3} + \delta\right) \bar{\tau}^2\right]}{\int_{-\infty}^{\bar{\tau}} \exp\left[-\frac{1}{2}(3\lambda - 1) \left(\epsilon + \frac{1}{3} + \delta\right) s^2\right] ds}, \quad (56a)$$

$$\bar{\gamma} = \frac{\left(\epsilon + \frac{1}{3}\right) \exp\left[-\frac{1}{2}(3\lambda - 1) \left(\epsilon + \frac{1}{3} + \delta\right) \bar{\tau}^2\right]}{\int_{-\infty}^{\bar{\tau}} \exp\left[-\frac{1}{2}(3\lambda - 1) \left(\epsilon + \frac{1}{3} + \delta\right) s^2\right] ds}. \quad (56b)$$

The solutions (56a, b) show that $\bar{\gamma}$ becomes exponentially small as $\bar{\tau} \rightarrow \infty$, whilst $\bar{\beta}$ increases, becoming linear in $\bar{\tau}$ as $\bar{\tau} \rightarrow \infty$. Thus, a further non-uniformity arises as $\bar{\tau} \rightarrow \infty$, in particular when $\bar{\tau} = O(K^{\frac{1}{2}})$, with $\beta = O(1)$ and γ exponentially small in K . To complete the solution we introduce region IV.

Region IV: $\tau > \tau_0 + O(K^{-\frac{1}{2}})$, $\beta = \beta_0(\tau) + o(1)$, $\gamma = o(K^{-n}) \forall n > 0$ as $K \rightarrow \infty$,

where $d\beta_0/d\tau = -\frac{25}{9}\{\beta_0 - (1 - 3\lambda)\}\{\beta_0 - \frac{1}{5}(1 + 3\epsilon)\}\{\beta_0 - \frac{1}{5}(1 + 3\epsilon + 3\delta)\}$, (57a)

subject to matching with the solution in region III as $\tau \rightarrow \tau_0$, which yields

$$\beta_0 \rightarrow 0 \quad \text{as } \tau \rightarrow \tau_0. \quad (57b)$$

The solution of the initial-value problem (57a, b) is readily obtained in implicit form (Billingham 1991). However, the behaviour of β_0 is again most easily determined by studying the form of equation (57a). There are two possibilities.

$$\frac{1}{3} < \lambda \leq \frac{1}{5}(2 + \epsilon)$$

In this case, β_0 is monotone increasing with τ , and $\beta_0 \rightarrow 3\lambda - 1$ as $\tau \rightarrow \infty$. This behaviour as $\tau \rightarrow \infty$ corresponds to case (ii) of the full initial-value problem above.

$$\lambda > \frac{1}{5}(2 + \epsilon)$$

Again, β_0 is monotone increasing in τ , and in this case $\beta_0 \rightarrow \frac{1}{5}(1 + 3\epsilon)$ as $\tau \rightarrow \infty$. This behaviour as $\tau \rightarrow \infty$ corresponds to case (iii) of the full initial-value problem above. This completes the asymptotic solution of the initial-value problem (32c-e) for $K \gg 1$ with $\epsilon, \delta = O(1)$.

For $\lambda > \frac{1}{5}$, region I is again a thin initial transient region where β becomes of $O(K^{-1})$. In region II, β increases slowly, whereas γ decreases more rapidly until β and γ are of $O(K^{-\frac{1}{2}})$ as the solution enters region III. In this region, γ becomes exponentially small in K , whereas β increases rapidly to become of $O(1)$. Region IV completes the solution and $\beta \rightarrow 3\lambda - 1$, $\gamma \rightarrow 0$ as $\tau \rightarrow \infty$ for $\frac{1}{3} < \lambda \leq \frac{1}{5}(2 + \epsilon)$, whereas $\beta \rightarrow \frac{1}{5}(1 + 3\epsilon)$, $\gamma \rightarrow 0$ as $\tau \rightarrow \infty$ for $\lambda > \frac{1}{5}(2 + \epsilon)$. This asymptotic structure corresponds to

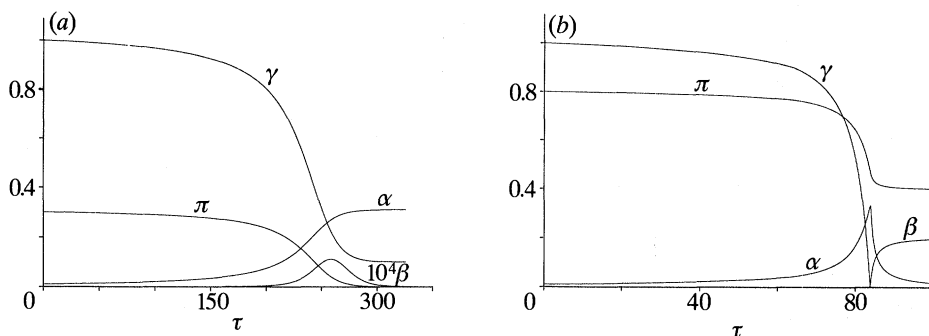


Figure 11. The solution of the initial-value problem (32) for $\epsilon = 0.01$, $\delta = 0.01$, $K = 1000$ and: (a) $\lambda = 0.3$, (b) $\lambda = 0.8$.

clock-like behaviour due to a type 2 reaction mechanism. Regions I and II make up the induction period, which has duration τ_0 , given by (54). Region III is a transition region where the concentration of the clock chemical, B, becomes significant, and region IV encompasses the final evolution of the concentrations β and γ to their equilibrium values. The numerical solution of the initial-value problem (32c–e) for $\lambda = 0.8$, $K = 1000$, $\delta = \epsilon = 1$ is illustrated in figure 10b. The asymptotic structure outlined above is clearly visible and $\tau_0 \approx 0.212$ is in good agreement with this numerical solution.

We have now shown that the solution of the initial-value problem (32c–e) can display clock-like behaviour in either of the cases $\epsilon \ll 1$, $K = O(1)$, $\lambda > 0$, due to a type 1 reaction mechanism and $\epsilon = O(1)$, $K \gg 1$, $\lambda > \frac{1}{3}$, due to type 2 reaction mechanism. Finally, we examine the form of solutions of the initial-value problem (32c–e) when $\epsilon \ll 1$ and $K \gg 1$ and we expect that clock-like behaviour will occur with both types of reaction mechanism acting on the system.

(c) *Asymptotic solution of the initial-value problem for $0 < \epsilon \ll 1$, $K \gg 1$*

We can determine the asymptotic form of the solution of the initial value problem (32c–e) for $0 < \epsilon \ll 1$ and $K \gg 1$ by considering the behaviour of the integral path S_0 (which represents the solution in the (β, γ) phase plane) under the two limiting processes $\epsilon \rightarrow 0$ and $K \rightarrow \infty$. For $\epsilon \ll 1$ the initial point $(0, 1)$ lies in the immediate neighbourhood of the equilibrium point $(0, 1 + 3\epsilon)$ and remains there for a time $\tau_0 = O(\epsilon^{-1})$ as $\epsilon \rightarrow 0$. The presence of the equilibrium point $(0, 1 + 3\epsilon)$ close to the point $(0, 1)$ represents the action of the type 1 reaction mechanism as $\epsilon \rightarrow 0$. For $K \gg 1$ the integral path S_0 lies close to the γ axis and for $0 < \lambda \leq \frac{1}{3}$ remains there with $\beta \rightarrow 0$, $\gamma \rightarrow 1 - 3\lambda$ as $\tau \rightarrow \infty$. However, for $\lambda > \frac{1}{3}$ the integral path S_0 lies close to the γ axis for $\tau \leq \tau_0 = O(1)$ as $K \rightarrow \infty$, and then lies close to the β axis for $\tau \geq \tau_0$, with $\beta \rightarrow 3\lambda - 1$, $\gamma \rightarrow 0$ as $\tau \rightarrow \infty$ for $\frac{1}{3} < \lambda \leq \frac{1}{5}(2 + \epsilon)$ and $\beta \rightarrow \frac{1}{5}(1 + 3\epsilon)$, $\gamma \rightarrow 0$ as $\tau \rightarrow \infty$ for $\lambda > \frac{1}{5}(2 + \epsilon)$. This is due to the form of equations (32c, d) for $K \gg 1$ which show that for $\beta > 0$ and $\gamma > 0$, β_τ and γ_τ are large and negative unless $\beta\gamma = O(K^{-1})$. This distortion of the integral paths of the system (32c, d) represents the action of the type 2 reaction mechanism as $K \rightarrow \infty$. When $\epsilon \ll 1$ and $K \gg 1$ the integral path will both originate in the immediate neighbourhood of the point $(0, 1 + 3\epsilon)$ and lie close to the axes in the (β, γ) phase plane. For $0 < \lambda \leq \frac{1}{3}$, β therefore remains uniformly small for $\tau \geq 0$ and no clock-like behaviour occurs as can be seen in the numerical solution for $\lambda = 0.3$, $K = 1000$, $\epsilon = \delta = 0.01$, illustrated in figure 11a. For $\lambda > \frac{1}{3}$ we expect that clock-like behaviour occurs and that the induction period has duration $\tau_0 = O(\epsilon^{-1})$ as $\epsilon \rightarrow 0$,

$K \rightarrow \infty$, since the time which the solution spends in the neighbourhood of the point $(0, 1 + 3\epsilon)$ is of $O(\epsilon^{-1})$, whereas the subsequent time which the solution takes to reach the β axis is of $O(1)$. The numerical solution for $\lambda = 0.8$, $K = 1000$, $\epsilon = \delta = 0.01$ is illustrated in figure 11*b*. By comparing figures 10*b* and 11*b*, with $K = 1$ and $K = 1000$, respectively, it is clear that when $K \gg 1$, $\epsilon \ll 1$ and $\lambda \geq \frac{1}{3}$, when the solution lies in the neighbourhood of the point $(0, 1 + 3\epsilon)$, the type 1 reaction mechanism is dominant, with the type 2 reaction mechanism only affecting the form of the solution close to the end of the induction period at $\tau = \tau_0 \approx 87$ in this case.

In this section, we have shown that the reaction scheme (26) behaves in a similar way to the scheme (1) for $\epsilon \ll 1$, $K = O(1)$ with the type 1 reaction mechanism dominant, and in a similar way to the scheme (4) for $\epsilon = O(1)$, $K \gg 1$ with the type 2 reaction mechanism dominant. When $\epsilon \ll 1$ and $K \gg 1$ the type 1 reaction mechanism is dominant during the induction period, whereas the rapid growth of the concentration of the autocatalyst, B, at the end of the induction period is due to the type 2 reaction mechanism.

4. Conclusion

In this paper we have examined how two completely different reaction mechanisms, induction and inhibition, can lead to clock reaction behaviour. We studied the effect of these mechanisms separately in two simple reaction schemes and also in a model for the iodate–arsenous-acid reaction. This model reaction scheme can exhibit induction and/or inhibition depending on the initial concentrations of the reactants. We found that, when these mechanisms co-exist, induction is dominant during the induction/inhibition period. For the schemes considered the analytical methods adopted in the paper have enabled us to obtain simple expressions for induction and inhibition times in terms of the parameters in the system. Moreover, this approach provides a systematic method for the qualitative and quantitative analysis of kinetic schemes for the possibility of clock reaction behaviour.

J. B. acknowledges the assistance of an S.E.R.C. Research Studentship. We are also grateful to Professor P. Gray (Gonville and Caius College, Cambridge) and Dr S. K. Scott (University of Leeds) for valuable discussions on the nature of chemical clock reactions.

References

- Barrett, R. L. 1955 *J. chem. Educ.* **32**, 78.
- Billingham, J. 1991 Travelling waves and clock reactions in quadratic and cubic autocatalysis. Ph.D. thesis, University of East Anglia, Norwich.
- Billingham, J. & Needham, D. J. 1991 *Phil. Trans. R. Soc. Lond.* A **334**, 1–24.
- Burrett, G. M. & Melville, H. W. 1947 *Proc. R. Soc. Lond.* A **189**, 456.
- Candy, T. E. G., Hodgson, M. & Jones, P. 1992 *J. chem. Soc. Perkins Trans. II*. (In the press.)
- Chien, J. 1948 *J. Am. chem. Soc.* **70**, 2256.
- Cooke, D. O. 1979 *Inorganic reaction mechanisms*. London: The Chemical Society.
- Dainton, F. S. 1966 *Chain reactions: an introduction*. London: Methuen.
- Dushman, S. 1904 *J. phys. Chem.* **8**, 453.
- Field, R. J. & Noyes, R. M. 1974 *J. chem. Phys.* **60**, 1877.
- Gowland, R. J. & Stedman, G. 1983 *J. chem. Soc. chem. Commun.* 1038.
- Gray, P., Griffiths, J. F. & Scott, S. K. 1984 *Proc. R. Soc. Lond.* A **397**, 21.
- Gray, P. & Scott, S. K. *Chem. Engng Sci.* **38**, 29.
- Haggett, M. L., Jones, P. & Oldham, K. B. 1963 *J. chem. Educ.* **40**, 367.
- Phil. Trans. R. Soc. Lond.* A (1992)

- Hanna, A., Saul, A. & Showalter, K. 1982 *J. Am. chem. Soc.* **104**, 3838.
- Jones, P., Haggett, M. L. & Longridge, J. L. 1964 *J. chem. Educ.* **41**, 611.
- Jones, P. & Oldham, K. B. 1963 *J. chem. Educ.* **40**, 366.
- Lambert, J. L. & Fina, G. T. 1984 *J. chem. Educ.* **61**, 1037.
- Liebhavsky, H. A. & Roe, G. M. 1979 *Int. J. chem. Kinet.* **11**, 693.
- Merkin, J. H., Needham, D. J. & Scott, S. K. 1986 *Proc. R. Soc. Lond A* **406**, 299.
- Roebuck, J. R. 1902 *J. phys. Chem.* **6**, 365.
- Scott, G. 1965 *Atmospheric oxidation and antioxidants*. Amsterdam: Elsevier.

Received 31 October 1991; accepted 18 March 1992